Structural Eng./Earthquake Eng. Vol. 9, No. 4, 227s—236s, January 1993
Japan Society of Civil Engineers (Proc. of JSCE No. 459/ I—22)

STIFFNESS EVALUATION OF SUBMERGED FLOATING FOUNDATION MOORED BY FOUR CABLES

Shigeru KURANISHI*, Tetsuo IWAKUMA**,
Shinjiro OHMOTO***
and Masatoshi NAKAZAWA****

As an application of cable structures to bridge structures, a submerged floating foundation moored by four cables is studied. The applied forces considered are the buoyancy, vertical load and horizontal force partly as a model of the tidal current. In order to examine the resistance against the overturn moment action, the governing equations with geometrical nonlinearity are solved by a direct integration method. As far as the sufficiently large tensile forces are introduced into all four cables, the system shows stable and almost linear responses, which may lead to a simplified design code generation based on a simple linear theory.
Key Words : Cable Structure, Submerged Floating Foundation

1. INTRODUCTION

Cooperative constructions in the developing countries and development of natural resources near the polar circles are parts of the most important tasks recently assigned to civil engineers in our country. Such cases often require the construction under very severe conditions. For example in bridge construction over the deep sea, it is so difficult to secure rigid foundations that the span length of the bridges becomes long, and the cost becomes high. At the same time, such huge structures are likely to destroy the environment in the aesthetic sense. Considering such circumstances, introduction of submerged but stiff floating foundations not only removes such difficulties but also extends the freedom of designing.

Since the floating bodies are generally moored by cables, they are sensitive to the dynamic effects of wave and tidal current and show nonlinear mechanical behavior. Consequently the recent researches are mainly related to the nonlinear dynamic analysis of the floating and moored bodies including the effect of slack cables. However we here restrict our attention within studies of submerged floating bodies as a model of the floating foundation, which undergoes relatively small influence of surface waves. Therefore in order to carry out the feasibility study of such structures, the system is modeled by a rigid submerged body moored by a number of cables anchored on the sea bed. Only the static and elastic analyses are carried out to examine their spatial stiffness.

The major subject of studying such floating structures subjected to the buoyancy has been the so-called mooring problem[e.g.1),2)], and most systems have not been permanent structures nor foundations but floating bodies under construction. The complication caused by the nonlinear behavior of cables or chains which anchor the floating body in the water or the hydraulically dynamic effect like the tidal current and wave action may be the factors against development of such structural systems. In the analyses the large displacement analysis[3)] of the cable must be also taken into account, and the dynamic contact[4)] problem of cables at anchor may become important.

The buoyancy acting along the cable has been sometimes approximated by usage of the under-water weight, but it has been reported[5),6),7)] that such an approximation leads to significant discrepancies in the behavior and configuration of a long cable. Furthermore, in the analyses of complex system of structures in the water which usually use the static and/or dynamic FEM[e.g.4),8)], the buoyancy is often approximated by this under-water weight.

In this study, the system to be analyzed is so simple that a direct numerical integration of the boundary-value problem can be employed, where the effects of the buoyancy and tidal force are taken into account. The responses against the vertical loading has been extensively studied[7)], and it was found to be almost linear. We here examine the static responses against the overturn moment forces together with the effects of the vertical and horizontal loadings. The dynamic effect of waves is not included here since the floating body is completely submerged under the water and the effect is presumably sec-

* Dr.Eng. Professor, Tohoku University, Department of Civil Engineering (Aoba Sendai, 980).
** Ph.D. Associate Professor, Tohoku University.
*** M.Eng. Kumagai-Gumi K.K. Tsukuba Laboratory (1043 Onigakubo Tsukuba, 300-20).
**** Dr.Eng. Research Associate, Tohoku University.

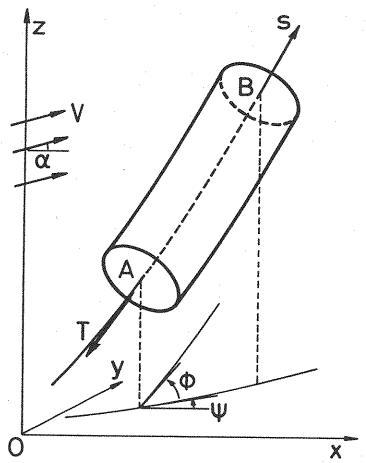

Fig. 1 Cable element and coordinate system

ondary. In the same sense, the dynamic nonlinearity at the anchor point is not considered here, either.

2. CABLE EQUATIONS

Since the governing equations considering the geometrical nonlinearity of cables in finite displacements have been already rationally formulated, we here simply enumerate them, and the non-dimensional parameters used in the present analyses are introduced.

The Cartesian coordinate system is defined as shown in **Fig.1** and s-axis is taken along the cable. Let ψ and ϕ denote the angles between the differential element ds and the x-z and x-y planes respectively. They are reckoned positive when they are counterclockwise as seen from the positive end of a coordinate axis, and are defined within the region of $0° \leq (\psi,\ \phi) \leq 180°$. The cable is elastic with its Young's modulus E following one-dimensional Hooke's law. Distortion of the cross section is neglected because the cable is relatively long, but the effect of elongation is taken into account.

(1) Buoyancy

Consider a differential element of a cable ds, and the hydrostatic pressure is directly acting only on its cylindrical side surface. No pressure is acting on the cross sections indicated by A and B in the figure, although the indirect action by the hydrostatic pressure on the end sections is naturally transmitted as a part of the cable tension T. Since Archimedes' principle indicates that the buoyancy is determined as a resultant force of the hydrostatic pressure action on the body, the buoyancy of this cable element ds is not uniform but varies along the cable axis. An often-used approximation using the under-water weight cannot take this effect into account and simply yields an average total buoyancy. Then the x-, y- and z-components of the buoyancy are simply calculated by geometrical and mechanical consideration as

$$dp_x = -A\gamma \cos\phi \sin\phi \cos\psi \left(1 + \frac{T}{EA}\right) ds \quad \cdots \text{(1-a)}$$

$$dp_y = -A\gamma \cos\phi \sin\phi \sin\psi \left(1 + \frac{T}{EA}\right) ds \quad \cdots \text{(1-b)}$$

$$dp_z = A\gamma \cos^2\phi \left(1 + \frac{T}{EA}\right) ds \quad \cdots \text{(1-c)}$$

where γ is the unit weight of fluid; A is the cross-sectional area of the cable; T is the cable tension. These equations express the distribution correctly, and indicate that the vertical portion ($\phi = \pi/2$) has no effect from the buoyancy except the component transmitted from the end sections of the cable.

(2) Tidal Force

Since the hydrodynamic effects are all neglected in this model, the tidal force is treated as a distributed force. Let the tidal current with stationary velocity V flow in the direction of the angle α from the x-z plane. As a simple model, the tidal force is assumed to be given by the Morison formula[8),9)]. The induced drag forces not only in the direction perpendicular to the cable axis but also in the tangential direction due to friction[4),5),10)] are considered here.

(3) Governing Equations

Geometrical and mechanical consideration leads to the equilibrium equations, kinematics and boundary conditions of the cable subjected to the force defined in the Sections (1) and (2). Then the governing equations are non-dimensioned to define appropriate parameters for case studies. Firstly, the independent variable s is normalized by the initial length of the cable, to introduce a new independent variable $\xi \equiv s/\ell$, and all the state quantities are considered as functions of ξ. The position vector of the axis is also non-dimensioned as

$$\eta_x(\xi) \equiv x(s)/\ell, \quad \eta_y(\xi) \equiv y(s)/\ell, \quad \eta_z(\xi) \equiv z(s)/\ell \quad \cdots \text{(2)}$$

The tensile stiffness EA of the cable is used to make the cable tension non-dimensional;

$$t(\xi) \equiv T/(EA) \quad \cdots \text{(3)}$$

Following these manipulation, we can define three essential parameters relating to its own weight per unit length, geometry and tidal force as

$$\zeta \equiv W/\gamma A, \qquad k_1 \equiv \gamma \ell/E$$
$$k_2 \equiv k_1 C_{DN} D V^2/(g A) \quad \cdots \text{(4)}$$

where ζ is a parameter concerning the cable weight per unit length W. C_{DN} is the drag coefficient in the direction perpendicular to the cable axis, and the ratio of the drag coefficients C_{DT} to C_{DN} will be

expressed by $C_{TN} \equiv C_{DT}/C_{DN}$. A cable-length parameter k_1 is given by the ratio of the total buoyancy of the entire cable and EA. A tidal-force parameter k_2 is defined by the fluid force per unit length of the cable in its perpendicular direction. D and g are the diameter of the cable and gravitational acceleration respectively.

Thus the field equations are given by a set of six simultaneous ordinary differential equations of the first order as follows:

$$\frac{d\phi}{d\xi} = \frac{1}{t}\Big\{k_1\,[\zeta - (1+t)]\,\cos\phi + \frac{1}{2}\,k_2\,(1+t)\,\cos(\psi-\alpha)\,\sin^2\phi\,|\cos(\psi-\alpha)|\Big\} \quad \cdots\cdots\cdots \text{(5-a)}$$

$$\frac{d\psi}{d\xi} = \frac{1}{t}\left\{\frac{1}{2\cos\phi}\,C_{TN}\,k_2\,(1+t)\times \sin(\psi-\alpha)\,|\sin(\psi-\alpha)|\right\} \quad \cdots\cdots\cdots \text{(5-b)}$$

$$\frac{dt}{d\xi} = \zeta\,k_1\,\sin\phi - k_2\,(1+t)\times \cos(\psi-\alpha)\,\cos\phi\,|\cos(\psi-\alpha)\,\cos\phi| \quad \cdots\cdots\cdots \text{(5-c)}$$

$$\frac{d\eta_x}{d\xi} = (1+t)\,\cos\phi\,\cos\psi \quad \cdots\cdots\cdots \text{(5-d)}$$

$$\frac{d\eta_y}{d\xi} = (1+t)\,\cos\phi\,\sin\psi \quad \cdots\cdots\cdots \text{(5-e)}$$

$$\frac{d\eta_z}{d\xi} = (1+t)\,\sin\phi \quad \cdots\cdots\cdots \text{(5-f)}$$

The geometrical boundary conditions may be specified at the end points;i.e.

$$\eta_x = \overline{\eta}_x, \qquad \eta_y = \overline{\eta}_y, \qquad \eta_z = \overline{\eta}_z \quad \cdots\cdots\cdots (6)$$

where, $\overline{\eta}_x$, $\overline{\eta}_y$ and $\overline{\eta}_z$ are the non-dimensional position vector components of the end points of the cable. On the other hand, the force boundary conditions can be given by the equilibrium of the cable tension and the applied end forces as follows:

$$f_x = \nu\,t\,\cos\phi\,\cos\psi \quad \cdots\cdots\cdots \text{(7-a)}$$

$$f_y = \nu\,t\,\cos\phi\,\sin\psi \quad \cdots\cdots\cdots \text{(7-b)}$$

$$f_z = \nu\,t\,\sin\phi \quad \cdots\cdots\cdots \text{(7-c)}$$

where f_x, f_y and f_z are non-dimensional x-, y- and z-components of the external forces, F_x, F_y and F_z divided by EA respectively; ν is defined as the inner product of outer unit normal vector and unit vector along s-axis at the terminal cross sections, and takes the values -1 at $s = 0$ and $+1$ at $s = \ell$. Note that, at the anchored points, the anchoring force must be calculated as addition of this end force $\boldsymbol{F}$ and the total hydrostatic pressure acting on the section.

3. ANALYSIS OF SUBMERGED FOUNDATION MOORED BY MULTIPLE CABLES

(1) Model

A submerged foundation is modeled as a rigid floating body moored by a certain number of cables anchored on the sea bed. The floating body itself is free to move in the three-dimensional space. Fundamental states of the problem can be summarized as follows:

1. The floating body is a rigid sphere and is submerged completely in the water. A constant buoyancy is modeled as an upward force which is kept acting vertically and constantly through the center of the body.

2. The lower ends of the cables are anchored directly on the sea bed, while the upper ends are attached through hinges on the equator of the floating sphere.

The main objective of this study is to examine the resistance characteristics of such a system subjected to the external action from the superstructure erected on the floating body. Therefore such actions must include not only the forces given in Eq.(7) but also the moment forces or forced rotations.

(2) Boundary Condition

Suppose that a floating body is moored by n cables. Then the boundary conditions at the anchored points are simply given from Eq.(6) by specifying their positions as

$$\eta_{xi} = \overline{\eta}_{xi0}, \qquad \eta_{yi} = \overline{\eta}_{yi0}, \qquad \eta_{zi} = \overline{\eta}_{zi0} \quad \cdots\cdots (8)$$

where, for example, each η_{xi} denotes η_x of the i-th cable ($i = 1, \cdots$ n), and $\overline{\eta}_{xi0}$ expresses the corresponding coordinate.

At the floating body, the boundary conditions of each cable are coupled. When only the forces in three directions are specified, Eq.7 must be replaced by

$$f_x = \sum_{i=1}^{n} t_i \cos\phi_i \cos\psi_i \quad \cdots\cdots\cdots \text{(9-a)}$$

$$f_y = \sum_{i=1}^{n} t_i \cos\phi_i \sin\psi_i \quad \cdots\cdots\cdots \text{(9-b)}$$

$$f_z = \sum_{i=1}^{n} t_i \sin\phi_i \quad \cdots\cdots\cdots \text{(9-c)}$$

where the subscript i indicates the cable number.

As mentioned earlier, the body is also subjected to the external moment action. Considering that the objective of this study is to get the stiffness of the total system, we will specify the rotation of the floating body instead of applying the moment forces. Namely the displacement control is adopted for simplicity of the numerical calculations. For example, suppose the connecting point of the first cable at the floating body as a reference point, and the relative position of the connecting points of the other cables are expressed by

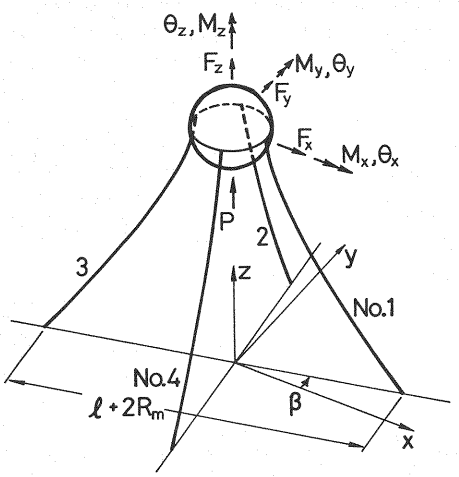

Fig. 2 Model and applied loads

$$\eta_{xi1} = \eta_{x11} + \Delta\eta_{xi} \quad \cdots\cdots\cdots\cdots\cdots\cdots \quad (10\text{-a})$$
$$\eta_{yi1} = \eta_{y11} + \Delta\eta_{yi} \quad \cdots\cdots\cdots\cdots\cdots\cdots \quad (10\text{-b})$$
$$\eta_{zi1} = \eta_{z11} + \Delta\eta_{zi} \quad (i = 2, \cdots n) \quad \cdots\cdots\cdots \quad (10\text{-c})$$

where $\Delta\eta_{xi}$'s denote the corresponding components of the relative distance from the reference point at the rotated configuration. These relative distances can be easily calculated geometrically, because the form of the body is sphere.

When the forced rotation is specified, the corresponding moment forces are also easily computed as reaction forces. Let r_{xi}, r_{yi} and r_{zi} denote the distances from the center to the action lines of the cable tensions, and the components of the moment force of the floating sphere are calculated by

$$M_x = \sum_{i=1}^{n}(t_{zi}\, r_{yi} - t_{yi}\, r_{zi}) \quad \cdots\cdots\cdots\cdots\cdots \quad (11\text{-a})$$
$$M_y = \sum_{i=1}^{n}(t_{xi}\, r_{zi} - t_{zi}\, r_{xi}) \quad \cdots\cdots\cdots\cdots\cdots \quad (11\text{-b})$$
$$M_z = \sum_{i=1}^{n}(t_{yi}\, r_{xi} - t_{xi}\, r_{yi}) \quad \cdots\cdots\cdots\cdots\cdots \quad (11\text{-c})$$

where t_{xi}'s indicate the components of the tension of the i-th cable at the connection.

(3) Method of Numerical Analysis

Since the field equations (5) hold in every cable, the set of $n \times 6$ simultaneous ordinary differential equations are to be solved under the boundary conditions given by Eqs.(8) through (11). The simplicity of the structure allows us to use the direct integration method instead of approximations like FEM. The Milne method is employed for numerical integration, and the two-point boundary value problem is solved by an adjoint method of the shooting methods[11]. The number of divisions for integration is determined by a test analysis of a simple catenary, and the actual length of the segment between two adjacent integration points is set 1m in the present numerical examples. The accuracy of seven significant digits can be obtained by this choice.

4. NUMERICAL EXAMPLE

(1) Four Point Mooring

As an illustration, the floating body moored by four cables shown in **Fig.2** is analyzed. Six components of external force and moment force are also shown in the figure, and the forced rotations discussed above are denoted by θ_x, θ_y and θ_z. The buoyancy acting on the body minus its dead load is denoted by P. The angle β is introduced to consider the position relative to the superstructure. For example, the x-direction may be the longitudinal direction of the bridge structure. Among many choices for β, we here consider only the two extreme cases, one of which is when $\beta = \pi/4$ (Model A) and another is when $\beta = 0$ (Model B).

a) Floating Body

Design load from the superstructure is set 5,000tf (49MN), and the design buoyancy of the body P is calculated from this design load basing on the safety factor 2 to be 10,000tf (98MN). This amount of buoyancy can be introduced to the steel sphere if its diameter ($2 \times R_m$) is set 28m.

b) Cable

The parallel-wire strand cable with uniform cross-section is employed, because it undergoes relatively small cross-sectional distortion. Its Young's modulus is 2.0×10^6kgf/cm^2 (196GN/m^2). The effective cross-section which resists the tensile force is set 58.88% of the actual area[12], and is used to calculate the elongation and stresses numerically. Note that the actual area is used for the non-dimensional expressions of the results in the following sections. The tensile strength of the piano wire is 140kgf/mm^2 (1.37GPa) and the strength correction factor of the cable for individual strength of the wire is set 0.95. Finally with the safety factor 1.5, the maximum 10,000tf of the cable tension determines the diameter of the cable, D=0.3m. The cable weight W/A is set 4.62gf/cm^3 (45.3kN/m^3).

The depth of the continental shelf suggests likely values of the length of cables to be between 100 and 200m. Moreover the results[7] obtained in the two point mooring problems indicate that, the longer the cables are, the less becomes the maximum buoyancy or the maximum capacity of the vertical loading from the superstructure. On the other hand, the shorter the cable length becomes, the more effect from the tidal current the system has on its configuration. Therefore the distance between the diagonally opposite points of anchorage are set equal to the initial

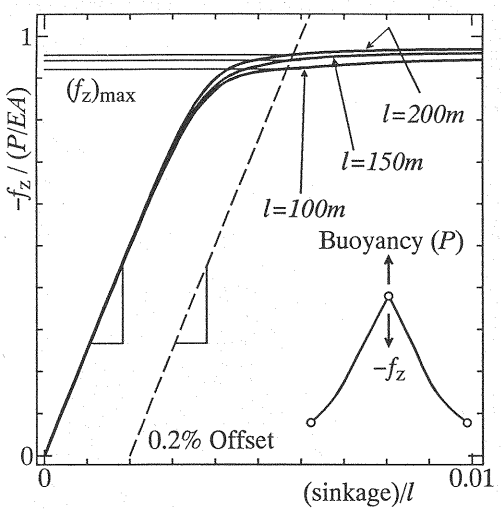

Fig. 3 Maximum loading capacity

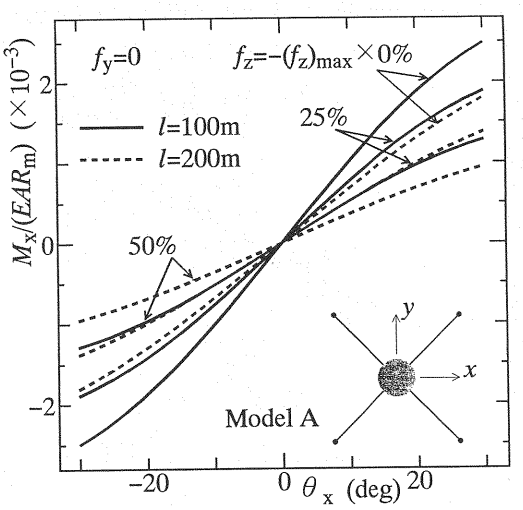

Fig. 4 Effect of vertical load on rotating stiffness about x-axis (Model A)

length of the cable plus the diameter of the floating body. The cyclic loadings and deterioration by creep and corrosion are not taken into account.

c) Fluid Force

The average velocity of the tidal current in the neighboring seas of Japan is usually less than 2m/s, but in the special areas like the Naruto Narrows[9], it sometimes exceeds 5m/s. Considering this situation, we employ 5m/s as the maximum velocity of the tidal current. The unit volume weight of the sea water γ is 1.02 gf/cm^3 (9.8kN/m^3) and the values C_{DN} = 1.2 and C_{DT} = 0.015 on rough surface are used.

(2) Load Carrying Capacity

In order to get the maximum load carrying capacity of the system as a representative parameter for the strength, the two-dimensional analyses have been carried out to obtain the relations between the vertical load and sinkage of the floating body. The cable length ℓ is set 100m, 150m or 200m, and the corresponding k_1 parameter in Eq.(4) takes the values 5.1×10^{-6}, 7.56×10^{-6} and 1.02×10^{-5} respectively. The results are plotted in **Fig.3** and show that the linear responses are obtained as long as the vertical load is approximately less than 80% of the buoyancy in all cases. Beyond that point the structure abruptly loses its stability, but the critical loads are different in each case depending on the length of the cable. In order to define the maximum capacity, we use the 0.2% offset method which is often employed to define a yield stress of materials without clear yield point. Then the maximum load carrying capacity $(f_z)_{max}$ is determined as follows:

$EA(f_z)_{max}$ = 9700tf, (95.0MN) at ℓ = 100m
$EA(f_z)_{max}$ = 9550tf, (93.6MN) at ℓ = 150m
$EA(f_z)_{max}$ = 9400tf, (92.1MN) at ℓ = 200m

(3) Application of Moment about x-axis

As a simple application, let x-axis lie along the longitudinal axis of the bridge structure, and consider the case where the wind force or tidal current is acting in the transverse (y-) direction. The actions from the superstructure are modeled by a vertical load f_z and a forced rotation θ_x. Therefore the other boundary conditions of the floating body can be expressed as

$$M_y \equiv 0, \quad M_z \equiv 0$$

and they are kept all through the deformation.

a) Influence of Vertical Load

Typical resistance characteristics against the overturn moment for the Model A are shown in **Fig.4**, where the level of applied vertical load is indicated. The ordinate expresses the overturn moment nondimensioned by the tensile rigidity of the cable and radius of the floating body. The longer the cables are, the softer the response becomes. The stiffness decreases as the vertical load approaches to the buoyancy. However, the response is approximately linear up to rather large rotational angle as 20 degrees. The nonlinearity is relatively mild, and the change of the stiffness is monotonic.

Fig.5 shows responses of the Model B. The behavior is qualitatively similar to that of the Model A, but the nonlinearity becomes more significant as the

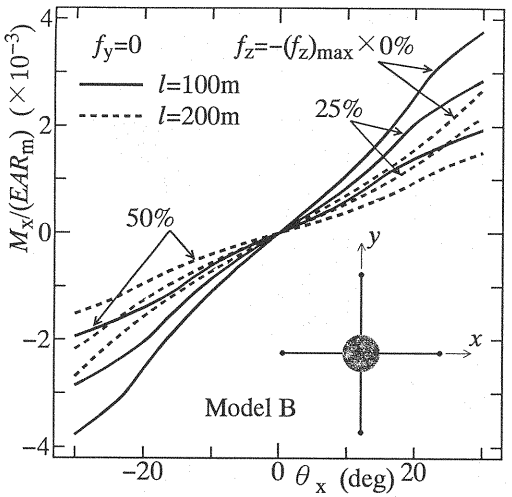

Fig. 5 Effect of vertical load on rotating stiffness about x-axis (Model B)

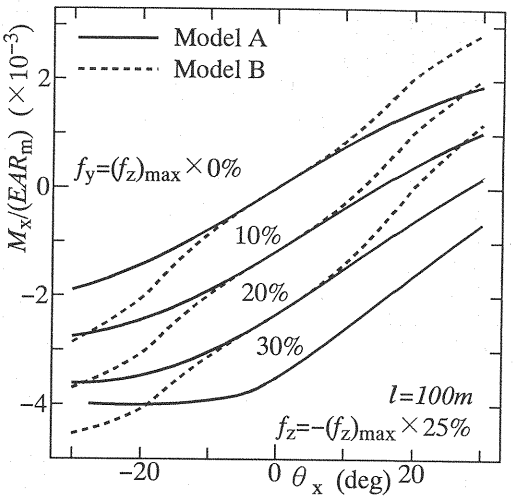

Fig. 6 Effect of horizontal load on rotating stiffness about x-axis

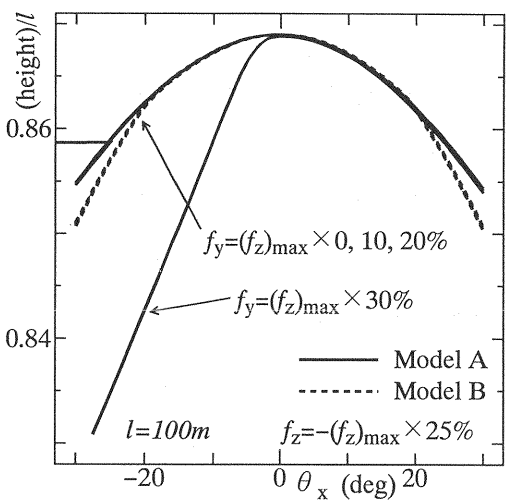

Fig. 7 Sinkage due to overturn moment

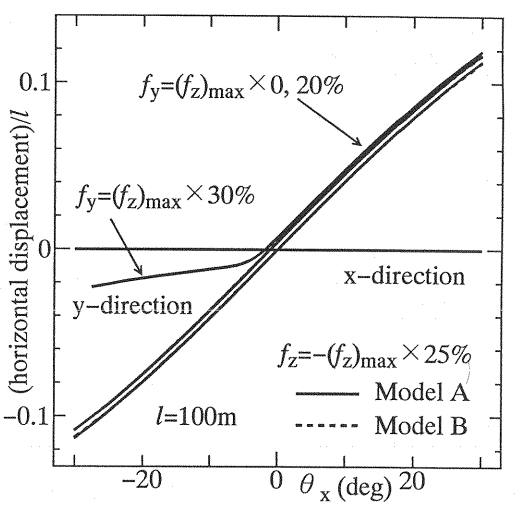

Fig. 8 Horizontal displacement of floating body

length becomes shorter. The stiffness of the system first becomes larger than the initial one temporarily, but, for example, the system with cables of 100m begins to soften as the rotation approaches to 20 degrees. Although this behavior may suggest that this nonlinearity stems from some kind of bifurcation, no such a complicated nonlinearity appear in the history of the horizontal displacements. It turns out that the cause of this behavior is related to redistribution of cable tensions in each of the cables, and it will be discussed later on.

b) Influence of Horizontal Load

The horizontal load considered here includes the fluid force acting on the floating body by the tidal current. The total force reaches 1,000tf (9.8MN) for the sphere of this size when the velocity of the current is 5m/s, but it is approximately 10% of the maximum load carrying capacity. Therefore at most 30% of the capacity is applied for the present study.

The influence of the horizontal load on the resistance against the tilting moment is shown in **Fig.6** for two models, and **Fig.7** shows the vertical motion in terms of the height of sphere from the sea bed non-dimensioned by the cable length.

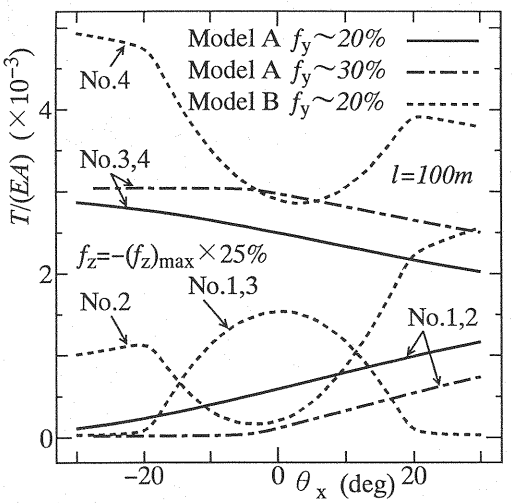

Fig. 9 Change of cable tensions

It is clear that the horizontal load increases the rotational angle of the floating body on which no moment force is applied. The body rotates more than 30 degrees when the horizontal load reaches 30% of the maximum capacity. However, the vertical displacement remains within a few percent of the cable length as shown in **Fig.7**. On the other hand, **Fig.8** indicates that the horizontal displacement becomes about 10%. Unlike other relations, the vertical motions are more or less the same for both models with different horizontal loads.

The moment required to make the body horizontal ($\theta_x = 0$) increases in proportion to the horizontal load, and, at this horizontal position, the sinkage becomes minimum and the stiffnesses of the two models coincide with each other. At other states of configuration the Model B is stiffer than the Model A, but the sinkage becomes larger. The Model A loses its stiffness rapidly as the horizontal load increases. For example, the resisting moment cannot exceeds a certain level and the slope becomes almost zero. At this stage the body sinks tremendously but the horizontal displacements remain very small as seen in **Fig.8**.

In order to explain the substantial cause of the nonlinearity shown above, the cable tensions are examined at each step of loading and are shown in **Fig.9**. As is clear from the boundary conditions, the Model A always keeps the cable tensions of No.1(3) and 2(4) identical. The change of those of the Model A is monotonic, and the tension of No.1 cable becomes almost zero when the horizontal load is 30% of the maximum capacity which is indicated by the dash-dotted lines. This is the cause of loss of stiffness, and thus the state can be interpreted as an ultimate state rather than a bifurcated path.

On the other hand, the loading Model B allows that the three cables have different cable tensions while No.1 and 3 undergo the same tension. Accordingly they show complicated changes as are depicted in **Fig.9**. Although the cables No.1 and 3 lose their tensions at a certain level of loading, the remaining cables keep resisting to the tilting moment in the plane of these two cables, and the system yields apparently high stiffness. It is quite likely that this state of deformation is unstable, but no further investigation has been carried out, because our objective is to examine the stiffness of the system and no clear criterion for instability can be established yet.

In any case, since the stiffness of the system is mainly governed by the cable tension, the amount of the buoyancy P initially given to the floating body is the most important factor for the resistance characteristics of the system.

c) Influence of Tidal Current

The tidal current of the velocity up to 5m/s yields almost no influence on the response of the system, and the results are not shown here, because the difference of the results cannot be perceived within the scale in these figures. The changes in the configuration of the cables in equilibrium are also very small. Therefore we can conclude that, as long as the cable tensions are large enough as expected in the system considered, the effect of the tidal current on the cables is very small in comparison with that on the floating body. Note that the latter plays an important role on the stiffness and stability of the structure as discussed in the previous section.

(4) Moment Loading about y-axis

The stiffness against the rotational moment about the y-axis of the same system is examined next. For simplicity, the boundary conditions are given in terms of forced rotations. Namely, while the boundary conditions in the vertical and horizontal directions are given by the force conditions, the geometrical conditions are assigned about y-axis to specify the forced rotation of the floating body. Therefore the boundary conditions about other axes are also given by the geometrical conditions as

$$\theta_x = 0, \quad \theta_z = 0, \quad \rightarrow \quad M_x \neq 0, \quad M_z \neq 0$$

where the nonlinear coupling of the moment forces leads to non-zero values for all the moment components.

a) Influence of Vertical Load

The influence of the vertical load is shown in **Fig.10**. Two models with the same length of the cable have the identical initial stiffnesses. However the Model B shows relatively higher nonlinearity and becomes stiffer at the beginning than the Model A.

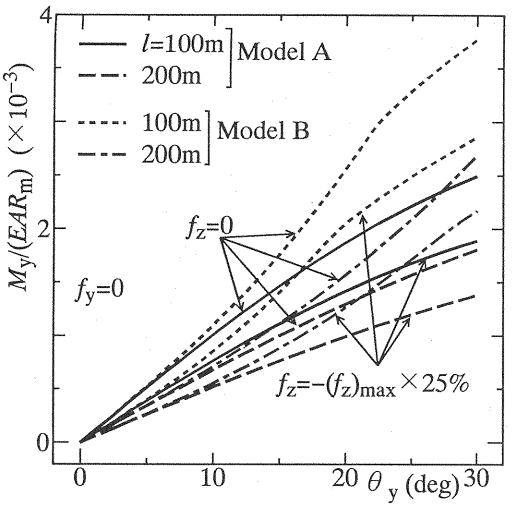

Fig. 10 Effect of vertical load on rotating stiffness about y-axis

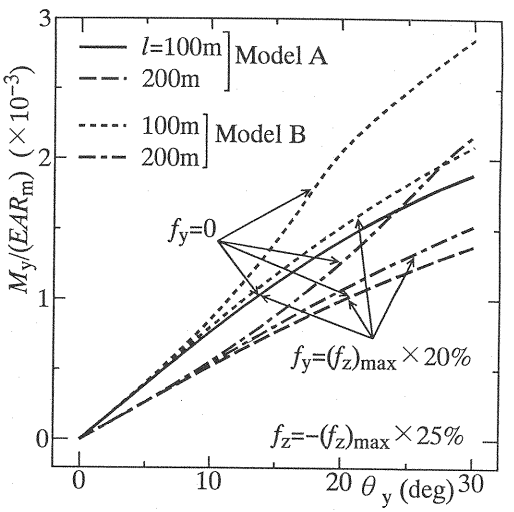

Fig. 11 Effect of horizontal load on rotating stiffness about y-axis

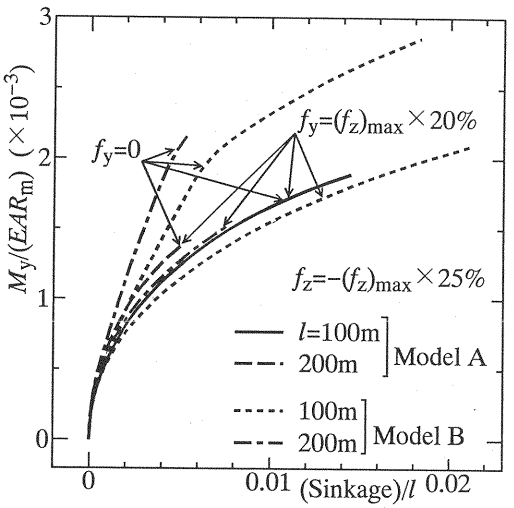

Fig. 12 Sinkage due to overturn moment about y-axis

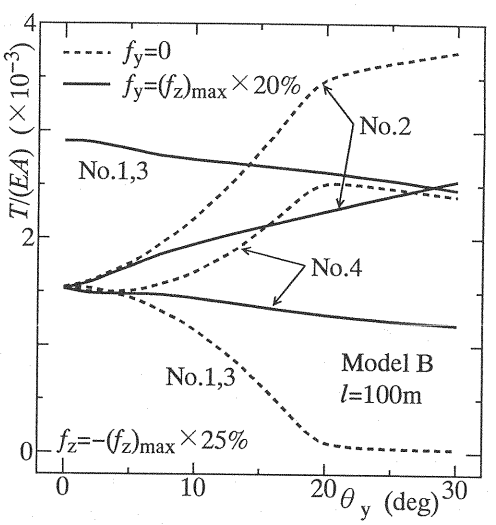

Fig. 13 Change of cable tensions

When the load approaches to a certain level, the Model B starts softening. The shorter the cable is, the more significant this tendency becomes. As for the Model A, the stiffness decreases monotonically as deformation progresses. Similarly to the results in the preceding sections, the vertical load has the effect to reduce the stiffness which substantially depends on the magnitude of the cable tensions.

b) Influence of Horizontal Load

Fig.11 shows a typical influence of the horizontal force in the y-direction. Under the boundary condition specified here, the Model A has almost no effect of this horizontal action and no difference is visible on the figure. The vertical motion of the floating body is plotted in **Fig.12** showing higher nonlinearity than that in Section (3), probably because of the complicated loadings.

For the Model B, there is observed no influence of the horizontal load as far as the initial stiffness is concerned, and the stiffness clearly decreases as the deformation increases. However it is of interest that the initially apparent nonlinearity disappears by the action of the horizontal load. **Fig.13** shows the corresponding changes of cable tensions. This figure suggests that this reduction of nonlinearity also stems from appropriate re-distribution of the

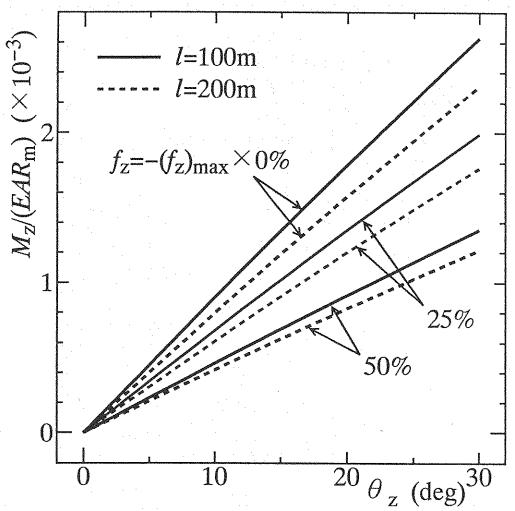

Fig. 14 Effect of vertical load on torsional resistance

tensions among four cables which becomes possible because of the non-zero moment components about all the three axes.

c) Influence of Tidal Current

No influence of the tidal current is observed in this case, either.

(5) Torsional Resistance

Again for simplicity the boundary condition at the floating body is specified geometrically as

$$\theta_x = 0, \quad \theta_y = 0, \quad \rightarrow \quad M_x \neq 0, \quad M_y \neq 0$$

which yields non-zero components of the three moment forces.

Unlike the cases in the Sections (3) and (4), the effects of the horizontal load and tidal current are not so big that one cannot distinguish the results on the figure. Furthermore the two loading models yield almost no difference. A significant discrepancy appears only on the results showing the effects of the vertical load in **Fig.14**. The behavior is completely linear, and it may be due to the states of high cable tensions.

5. CONCLUSION

The governing equations taking rationally into account the buoyancy and fluid force are solved to examine the stiffness of the submerged floating body moored by four cables. The results of a few case studies where emphasis is put on the resistance against the tilting moments are summarized as follows:

1. The relations between the moment forces and rotation about all the three axes are linear at their initial stage, and they become perfectly linear especially about the z-axis.

2. The application of the vertical and horizontal loads leads to the decrease of tension in some cables, and generally reduces the stiffness. However their effects are small as long as the loading levels are restricted within 30% of the load carrying capacity of the system.

3. Since the initial cable tensions are set approximately 25% of the strength, the final stage with almost zero stiffness has been achieved when the tension of two cables approaches to zero. However no abrupt drop of the stiffness nor softening have been observed.

4. The tidal force on the cables themselves in particular is a minor influence factor for the behavior of the floating body.

5. The sinkage by application of the moment loads shows nonlinear behavior but its absolute value is about one-tenth smaller than the horizontal displacements.

Accordingly, when the large initial buoyancy is introduced in the floating body so that the initial tension is set approximately 25% of the tensile strength of the cable, the responses of the system against the external moment forces are almost linear even though the tidal current is set at the highest level of the current specification, provided the vertical and horizontal forces are kept within 30% of the load carrying capacity of the system defined in Subsection 4.(2). Therefore it is expected that one can establish an easier approach of designing of such a structural system.

The studies left to be done are to use more realistic boundary conditions of the floating body specified only by the forces and moments, and to define the limit state of the system including bifurcation analyses. The limit state must also include the effect of the slack cables.

ACKNOWLEDGMENT This study has been supported in part by the Grant-in-Aid for Scientific Research from the Japanese Ministry of Education, Science and Culture under Grant No. 03452197 to Tohoku University.

REFERENCES

1) Ohmuro, T., Miyazaki, O. and Matsuda, E. : Static analysis of mooring cables subjected to tidal current. *Proc. of the Annual Conference*, JSCE, Vol.I, pp.184–185, 1975 (in Japanese).

2) Chang, P. and Pilkey, W. : The analysis of mooring lines. *Offshore Technology Conference*, No.OTC 1502, pp.II-845–854, 1971.

3) Ai, M., Nishioka, T. and Okumura, T. : A theoretical analysis of cable assembles. *Proc. JSCE*, JSCE, No.260, pp.17–32, 1977 (in Japanese).

4) Fukumoto, H., Nakanishi, H. and Namita, Y. : Dynamic response analysis of marine cable structure and its computational program. *Proc. JSCE*, No.356/I-3, pp.455–465, 1985 (in Japanese).

5) Maeshima, M., Kotoguchi, S. and Miki, T. : Analyses of marine cables. *Proc. of the Annual Conference*, JSCE, Vol.I, pp.216–217, 1990 (in Japanese).

6) Maeshima, M., Miki, T., Mizusawa, T. and Kotoguchi, S. : Dynamic analysis of tension leg platforms. *Proc. of the Annual Conference*, JSCE, Vol.I, pp.582–583, 1989 (in Japanese).

7) Fujii, M., Kuranishi, S. and Iwakuma, T. : A study of submerged floating foundation. *Proc. of the Annual Conference*, JSCE, Vol.I, pp.52–53, 1990 (in Japanese).

8) Lo, A. and Leonard, J. : Dynamic analysis of underwater cables. *J. Eng. Mech. Div., ASCE*, Vol.108, No.EM4, pp.605–621, 1982.

9) Horikawa, K. : *Coastal Engineering.* University of Tokyo Press, 1973 (in Japanese).

10) Berteaux, H.O. : Design of deep-sea mooring lines. *Marine Tech. Soc. J.*, Vol.4, No.3, pp.33–46, 1970.

11) Roberts, S.M. and Shipman, J.S. : *Two-Point Boundary Value Problems ; Shooting Method.* Elsevier, New York, 1972.

12) Japanese Road Association : *Specifications for Design of Highway Bridges*, 1980 (in Japanese).

(Received January 21, 1992)